SAN096-2937C
CONF-961113--1

GAS SENSING WITH ACOUSTIC DEVICES

S. J. Martin, G. C. Frye, J. J. Spates[1], and M. A. Butler

Microsensor Research and Development Department
Sandia National Laboratories
Albuquerque, NM, USA 87185-1425

Abstract

A survey is made of acoustic devices that are suitable as gas and vapor sensors. This survey focuses on attributes such as operating frequency, mass sensitivity, quality factor (Q), and their ability to be fabricated on a semiconductor substrate to allow integration with electronic circuitry. The treatment of the device surface with chemically-sensitive films to detect species of interest is discussed. Strategies for improving discrimination are described, including sensor arrays and species concentration and separation schemes. The advantages and disadvantages of integrating sensors with microelectronics are considered, along with the effect on sensitivity of scaling acoustic gas sensors to smaller size.

Introduction

Chemical sensors combine a chemical interface, which sorbs chemical species from the environment, with a physical transducer that provides an electrical output proportional to the amount of sorbed species (Fig. 1).

[1]On contract from Ktech Corporation, Albuquerque, NM 87110

DISCLAIMER

Fig. 1. Schematic of basic gas/vapor sensor showing concentration of analyte in the chemical interface.

Ideally, the chemical interface sorbs species rapidly and reversibly, maintaining a dynamic equilibrium between the ambient concentration and the concentration in the film. In this case, the sensor response provides real-time information about ambient chemical concentration.

Acoustic devices serve as a versatile "platform" for chemical sensing [1]. In the simplest cases, these devices are gravimetric sensors, responding to the mass of species accumulated in the sensing film. Since all species possess mass, any species that can be immobilized on the device surface can, in principle, be sensed. As a practical matter, however, species with lower volatility and/or stronger chemical interactions can be detected at lower concentrations using this technique.

The high mass sensitivity of acoustic sensors enables good chemical sensitivity to be achieved: mass changes in the picogram range or below can be detected and ppm to ppb detection levels have been reported for gas and vapor sensors [1,2]. The main difficulty with acoustic chemical sensors is achieving selectivity. The large number of chemical species that can be present in the environment and the difficulty in selectively sorbing these species on the detection surface, makes selective detection difficult. This difficulty can be partly overcome through design of the sensor system. There are several strategies for increasing selectivity. One approach is to fabricate an array of sensors, each having a different partially selective film, and using a pattern-recognition algorithm to identify the species present. Another approach is to add a "front end" to the sensor, such as a chromatographic column, that separates the species and enables identification based on their time of arrival at the sensor.

In order to shrink the size and cost, sensors are increasingly being fabricated on semiconducting substrates (e.g., Si or GaAs) and integrated with electronics. High volume sensors, such as pressure sensors and accelerometers, have followed this trend. For some applications, it may be advantageous to integrate gas and vapor sensors with on-chip electronics also. The reduction in size will enable sensor arrays to be fabricated in small packages and to be combined with electronics to monitor the sensor responses and execute pattern-recognition algorithms. Ultimately, it may be possible to integrate means for sample handling and species separation, enabling a complete "chemical analysis laboratory on a chip."

Acoustic Sensing Devices

A number of acoustic devices have been coated with sensing films and used for gas and vapor detection. We begin by surveying these devices and assessing their relative merits for chemical sensors and for integration with microelectronics.

Bulk quartz resonators Coated bulk-wave resonators, operating in the thickness-shear mode, were demonstrated to function as organic vapor sensors by King in 1964 [3]. These devices, shown in Fig. 2a, consist of a polished AT-cut quartz wafer with circular electrodes patterned on both sides. These devices are electrically excited into a fundamental resonance mode at a frequency for which the wafer thickness is twice the acoustic wavelength. These single-port devices are typically instrumented for sensor applications in an oscillator circuit that tracks the impedance phase, following either the series- or parallel-resonant frequency. Sauerbrey showed that changes in surface mass, caused by sorption, result in a change in resonant frequency [4]:

$$\Delta f = -\frac{2 f_o^2 \rho_s}{(\mu_q \rho_q)^{1/2}} \qquad (1)$$

where f_o is the unperturbed resonant frequency, ρ_s is surface mass density (mass/area), while μ_q and ρ_q are shear stiffness and density of the quartz. Eq. 1 was derived assuming the film remains acoustically thin and moves synchronously with the oscillating resonator surface. Researchers have shown that some films, for example polymers, may be soft enough to undergo significant deformation across the film, leading to a more complicated relationship between mass changes and resonant frequency [5].

Fig. 2. Bulk wave resonators: (a) discrete device using piezoelectric single-crystalline quartz; (b) integrable device fabricated on silicon using a piezoelectric (ZnO or AlN) film and bulk micromachining techniques.

Typical discrete resonator sensors (Fig 2a) use electrodes that are 5 - 10 mm across and a quartz thickness of 0.15 - 0.30 mm, yielding operating frequencies of 5 - 10 MHz. Device Q values are typically 10,000 - 20,000, leading to high oscillator stability. Micromachining techniques have been used, however, to fabricate arrays of bulk wave resonator sensors; these have been combined with oscillator circuitry fabricated on a silicon chip to form a hybrid resonator sensor array [6].

Eq. 1 indicates that mass sensitivity can be increased by using very thin devices that

operate at high frequency. In discrete resonators, this results in fragile devices that are difficult to fabricate and handle. Lakin *et al.* have used piezoelectric films and bulk Si micromachining techniques to form a high frequency bulk wave resonator, as shown in Fig. 2b [7]. An extensional-mode resonance is excited in a 5 μm thick, 0.5 mm long piezoelectric AlN membrane by electrodes deposited on the top and bottom. The membrane is formed by first sputter depositing the layer on a silicon wafer, then anisotropically etching silicon from the under side. The silicon substrate forms a "frame" that supports the fragile membrane. The resonant frequency is near 1 Ghz, with Q-values in the range 300 - 1000 [7]. From Eq. 1, this high fundamental resonant frequency produces extreme mass sensitivity (Table I). Recently, a distributed reflector array, consisting of alternating layers of materials with different acoustic impedance, has replaced the back etch as a means to acoustically isolate the device from the substrate.

Surface acoustic wave (SAW) device White *et al.* demonstrated in 1965 that a SAW could be electrically excited and detected in a piezoelectric substrate using an interdigital transducer [8]. This led to acoustic devices whose planar electrode pattern could be defined using photolithographic means, as shown in Fig. 3a. The operating frequency of the SAW is determined not by the wafer thickness, but by the transducer periodicity: $f = v/\lambda$, where v is the SAW propagation velocity and λ is the transducer periodicity (equal to acoustic wavelength at the transducer center frequency). Changes in surface mass result in changes in wave propagation velocity [1]:

$$\frac{\Delta v}{v_o} = -c_m f_o \rho_s \qquad (2)$$

where c_m is a substrate-dependent constant (1.29 x 10^{-6} cm^2-s/g for ST-cut quartz) and f_o is the operating frequency. When used in an oscillator circuit, relative changes in velocity are reflected as equivalent changes in fractional oscillation frequency, f: $\Delta f/f_o = \Delta v/v_o$. Since the SAW displacement decays exponentially with distance into the surface, and this decay length is proportional to frequency, Δf is proportional to f^2. There are other mechanisms, besides mass loading, whereby absorbed species can give rise to a sensor response; these included changes in viscoelastic properties [9] and electrical conductivity [10] induced by sorbed species.

Fig. 3. Discrete surface acoustic wave (SAW) sensors: (a) delay-line configuration; (b) two-port resonator.

Several researchers have also used the SAW resonator (Fig. 3b) as a sensing device [11]. This device consists of a pair of interdigital electrodes positioned in a resonant cavity formed by two distributed SAW reflector arrays patterned on the crystal surface. These reflector arrays consist of half-wavelength-wide metal strips or grooves; when the surface wave is incident on these periodic structures, the small amount of wave energy reflected from each discontinuity adds constructively to give nearly complete reflection (> 99%). The high Q and low insertion loss that results make these devices extremely stable when incorporated in an oscillator circuit, resulting in lower detection limits. However, the reflector arrays add significantly to the substrate area occupied by the sensor and complicate coating of the device surface.

SAW devices have been fabricated on silicon, using piezoelectric ZnO and AlN films.

These devices has also been constructed on piezoelectric GaAs substrates, without the need for a piezoelectric film. Fabricating these devices on semiconducting substrates enables them to be integrated with electronic circuitry to operate the device as a sensor. For devices fabricated on silicon, high temperature stability can be achieved by tailoring the thickness of the oxide layer. The high operating frequency of the SAW device, typically 100-500 MHz, complicates the design of integrated oscillator circuitry.

Flexural plate wave (FPW) device White *et al.* [12] have shown that a FPW device can be constructed on silicon and function as a sensitive chemical detector. As shown in Fig. 4, this device consists of a thin multilayer membrane, of which one layer is a piezoelectric material such as ZnO. Waves are excited and detected using interdigital transducers, as in the SAW device. Since the wave velocity in the membrane is much less than in a solid substrate, operating frequency is much lower (for a given transducer periodicity) than in the SAW device. This results in simpler oscillator electronics. Also, since the device is fabricated on silicon, it can be integrated with on-chip electronics [13]. FPW propagation velocity changes with surface mass as [12]:

$$\frac{\Delta v}{v_o} = -\frac{\rho_s}{2M} \tag{3}$$

where M is the mass/area of the FPW membrane. The confinement of acoustic energy in the thin membrane results in a very high mass sensitivity (Table I). While the backside etch required to construct the suspended FPW membrane is a difficult fabrication step, it allows the sensing film to be deposited on the opposite side from the transducer and oscillator electronics. This helps

solve a difficult packaging problem with sensors: how to expose the sensing region to the environment, while isolating the electronics.

Fig. 4. The flexural plate wave (FPW) sensor uses a piezoelectric ZnO film and interdigital transducers to excite flexural waves in a thin membrane.

A recent modification of the FPW device being investigated at Sandia National Laboratories is the magnetically-excited FPW (Mag-FPW) resonator, shown in Fig. 5. This consists of an insulating silicon nitride membrane suspended within a crystalline silicon. A meander-line transducer is patterned from metal on the membrane surface (Fig. 5a). Alternating current flowing in the transducer interacts with a static in-plane magnetic field to generate time-varying Lorentz forces, $\vec{f}$ (Fig. 5c). These deform the membrane, exciting it into a resonant mode. To efficiently excite the mode, the current lines of the transducer must be positioned along lines of maximum mode displacement (Fig. 5c). This requires a critical alignment between the top metallization pattern and the back-side etch mask. Both single-port and dual-port devices have been fabricated. The mag-FPW resonator exhibits Q-values of 8,000 in vacuum, dropping to about 1,000 in air. A unique feature is the ability to magnetically tune the transducer coupling to the resonant mode. Magnetic excitation requires an externally-applied magnetic field, but eliminates the need for a piezoelectric layer which frequently contains elements (e.g., Pb or Zn) that pose contamination problems in integrated circuit fabrication.

Fig. 5. The magnetically-excited flexural plate wave resonator uses the interaction between current in a meander-line transducer and an in-plane magnetic field to generate Lorentz forces that excite a resonant membrane mode.

Thin Rod Sensors Viens *et al.* have excited and detected acoustic waves in 25 μm-diameter metallic fibers and used these fibers as gravimetric gas and vapor sensors [14]. The fibers, constructed of Au or Cu, are coated around the periphery with a chemically sensitive film. Waves are excited in the fiber using a 2 MHz PZT compressional wave transducer, with energy coupled into and out of the fiber using hollow glass horns (see Fig. 6). Either extentional or flexural waves can be excited in the fiber, depending upon the orientation of the horn with respect to the fiber. The fractional change in wave velocity in the fiber due to surface mass ρ_s is [14]:

$$\frac{\Delta v}{v_o} = -\frac{\rho_s}{J\rho_1 a} \tag{4}$$

where ρ_1 and a are the density and diameter of the fiber; $J = 1$ for extensional waves and 2 for flexural waves. Eq. 4 considers only the effect of mass loading; a more complete analysis includes elastic effects in the film [14].

Fig. 6. The thin rod acoustic sensor uses compressional wave transducers to excite and detect waves in a thin metallic fiber.

By confining acoustic energy in a waveguide of extremely small cross-sectional area, the

thin rod sensor is extremely sensitive to surface mass perturbations: mass sensitivities of 95 cm^2/g have been measured [14]. Moreover, these high sensitivities are achieved at low operating frequencies. Disadvantages of this device include the lack of monolithic construction and the relative difficulty in coating the round, rather than planar, waveguide.

Cantilever-beam resonator Thundat *et al.* have employed micromachined cantilever beams (Fig. 7) that are electrically excited into resonance as chemical sensors [15]. The top surface of the cantilever is coated with a chemically sensitive film; as species are sorbed by the film, changes in mass and elastic constant serve to induce a change in the resonant frequency. The beam's resonant frequency is given by [15]:

$$f = \frac{1}{2\pi}\sqrt{\frac{K}{m*}} \tag{5}$$

where K and $m*$ are the effective spring constant and mass of the cantilever. These devices exhibit high mass sensitivity at low operating frequencies: 0.7 pg/Hz for an end-coated cantilever with a resonant frequency of 14 kHz. The cantilever beam experiences high losses when operated in air. Sniegowski reports Q-values for a 200 μm long, 40 μm wide cantilever that exceed 10^4 in vacuum, but drop to about 30 at 30 Torr; above this pressure, oscillation could not be sustained [16].

Fig. 7 The micromachined cantilever-beam resonator fabricated on a silicon substrate.

Since the micro-cantilever devices are constructed on silicon substrates, they can potentially

be integrated with electronic circuitry. In addition, the area occupied by the device is comparatively low; however, film deposition on the small beam surface is difficult. Since the signal level is fairly low, it would be advantageous to integrate control circuitry on chip to reduce parasitic capacitance.

Comb-drive resonator The comb-drive resonator consists of a poly-silicon mass suspended with poly-silicon springs that can oscillate laterally (in-plane) above the substrate surface (Fig. 8) [17]. This device uses electrostatic forces between interleaved combs to drive the suspended mass at its resonant frequency; a second set of combs is used to sense motion of the suspended mass based on changes in capacitance. The comb-drive resonator exhibits moderate mass sensitivity at low operating frequency (5 kHz typ.). As with the cantilever beam, the comb-drive resonator suffers from high losses due to air damping and signal levels are low so that the device would benefit from on-chip control electronics.

Fig. 7. The comb-drive resonator uses electrostatic forces between interleaved combs to excite and detect a polysilicon mass suspended by polysilicon springs.

Sensor Interfaces

In order to effect gas or vapor detection using acoustic devices, species from the gas phase (analytes) must be immobilized onto the surface where they can be detected gravimetrically. Since species in the gas phase enjoy a higher state of entropy than those adsorbed on a surface or dissolved in a film, there must be an attractive interaction between the gas-phase species and the

strength of this interaction increases (more negative ΔH_a), the number of sorbed species at a given concentration in the gas phase will increase; this results in greater sensitivity and a lower detection level.

Based on the above discussion, it would appear that stronger binding is always desirable. There is a tradeoff, however, between sensitivity and reversibility of the sensor. The average residence time, τ, that an adsorbed molecule stays on the surface is [18]:

$$\tau = \tau_o e^{-\Delta H/RT} \tag{7}$$

where τ_o is 10^{-12} to 10^{-13} s. Thus, when the gas phase concentration changes, the time to re-equilibrate the surface and sense the change in concentration increases as the binding energy increases.

The binding strength ΔH_a depends on the nature of the physical and chemical interactions occurring between an analyte and the surface. Species that undergo weak "physical" interactions, arising from van der Waals forces between molecules, have ΔH_a = 0.1 - 1 kcal/mole [1]. These species, said to be "physisorbed," are weakly bound ($\tau \sim 10^{-12}$ s) so that equilibrium between gas phase and bound species is rapidly achieved. Species that undergo chemical interactions, e.g., covalent or ionic bonding, have ΔH_a in the range of 20 - 40 kcal/mole (per bond) [1]. This results in a very long time constant ($\tau \sim 10^{17}$ s at room temperature when ΔH_a = 40 kcal/mole) and essentially irreversible binding. (Sensors exhibiting this behavior are typically termed "dosimetric" since their response indicates the total exposure of the sensor.) Since these chemical interactions are typically more specific than are physisorption-based interactions, better chemical selectivity can be achieved.

Using a simple Langmuir model for surface coverage, the equilibrium fraction θ of surface-sites occupied at a partial pressure P of the adsorbing species is given by [18]:

$$\theta = \frac{K_a P}{1 + K_a P} . \qquad (8)$$

Eq. 8 indicates that at low ambient concentrations (defined by K_a), the coverage and hence sensor response is linear with concentration; at high concentrations, response saturates at monolayer coverage. Thus, the range of concentrations over which the sensor responds depends on the equilibrium constant K_a. The mass per area arising from adsorption is $\rho_s = N_s \theta m$, where N_s is the number density of surface sites (approx. 10^{15} per cm^2) and m is the adsorbate mass.

Self-assembled monolayers One technique for chemically modifying the device surface is to coat the surface with a self-assembled monolayer (SAM) coating. These are typically alkane thiol molecules with a sulfer head group that binds strongly to a Au layer on the device surface. Due to the large number of relatively weak interactions between the hydrocarbon chains, the remainder of the molecule packs in semi-crystalline fashion on the surface to form exactly one monolayer. The tail group is accessible from the gas phase and determines the chemical properties of the surface. The SAM can be synthesized with various tail groups that have affinities for different analytes. Carboxylates, for example, has been shown to bind organophosphonate compounds [19], to which class nerve agents belong.

Porous films Bare surfaces and monolayer coatings result in rapid sensor response, but are limited in the total sensor response that can be produced by the monolayer coverage density. Porous films with high surface area can be deposited on acoustic sensors [3,20], giving a surface multiplication

factor of up to 50 or more. In addition, the chemistry of the porous surfaces can be modified to enhance the chemical interactions with the analyte of interest. If the film porosity is very small, with pore diameters of molecular dimension, enhanced uptake occurs due to the fact that a molecule is able to interact with more surface species. In recent work at Sandia National Laboratories, we have demonstrated that these microporous films can provide uptakes almost 100 times greater than with polymer films (see below) of similar thickness. In addition to providing greater surface area, these microporous materials can in some cases be tailored for size selectivity: small molecules are admitted while larger ones are excluded. This capability has been demonstrated using films containing small zeolite particles whose pore size is small enough to exclude larger analytes like iso-octane but provide effective concentration of smaller molecules like methanol and isopropanol [21].

Coordination/complexation chemistry To provide enhanced sensitivity as compared with simple physisorption-based sensors, chemical interactions arising from coordination and complexation chemistry can be used [2]. These interactions are strong enough to enable detection of gas phase species, but are generally not so strong that irreversible responses are observed. For example, a variety of researchers have used metal phthalocyanine compounds for sensitive detection of NO_2 [2,22], iodine [23], and aromatics [24]. These semiconducting compounds can provide both a mass and an acoustoelectric response [22]. Additional examples include Cook *et al.* [25], who demonstrated detection of SO_2 using organophosphine complexes, and Zellers *et al.* [26], who demonstrated the use of $PtCl_2$ complexes for sensitive and selective detection of styrene and butadiene.

Absorption-based sensors Films that absorb species into the bulk of the material are also useful

for chemical sensing. One class of materials is metal films: palladium has been used to detect hydrogen [27], while gold detects mercury [28]. For detecting organic vapors (environmental contaminants, workplace hazards, chemical warfare agents, explosives), many researchers have focused on the use of polymers as absorption-based films. The chemical properties of polymers can be altered by incorporating various functional groups along the carbon-chain backbone. Moreover, polymer films can be deposited easily by spin or spray casting from solution.

In absorption-based films, the gas-phase species are dissolved in the film; the quantity absorbed at equilibrium depends upon the *solubility* of the analyte in the film. This solubility, given by the partition coefficient K_p, depends on the change in enthalpy ΔH_a arising from solvation. Attempts have been made to predict the solubility of analytes in films. In the simplest model, the polymer and analyte are assumed to have no specific chemical interactions. Rather, the polymer is viewed as simply interacting physically with the analyte; the polymer is thus a collection of *nucleation* sites for analyte condensation. The following relationship was found between heat of condensation (ΔH_a) and (absolute) boiling temperature T_b of an analyte [29]:

$$\Delta H_a = 2950 - 23.7\, T_b - 0.02\, T_b^2 \ . \qquad (9)$$

Work by a number of researchers have shown that solubility in polymers can be predicted for a wide range of organic vapors from the analyte boiling point (Eqs. 6 and 9). It predicts that gases or vapors that are far above their boiling point at room temperature are difficult to absorb in a film. Thus, analytes that are normally gaseous at room temperature (e.g., methane, CO_2, and NO_2) are more difficult to detect (using physisorption processes) than are analytes that are normally liquid (e.g., benzene, and carbon tetrachloride).

A more sophisticated model for analyte solubility in polymers accounts for various physical interactions that can occur between the analyte and functional groups on the polymer backbone. The linear solvation energy relationships (LSER) postulate a linear relationship between the enthalpy change ΔH_a and various properties of the analyte and polymer [30]. From Eq. 6, this leads to:

$$\log(K_p) = c + rR_2 + s\pi_2 + a\alpha_2 + b\beta_2 + l\log(L) \qquad \textbf{(10)}$$

where c is a regression constant; parameters pertaining to the analyte include: R_2--the excess molar refraction, π_2--the dipolarity, $\alpha 2$--hydrogen-bond acidity; β_2--the hydrogen-bond basicity; L--the gas-liquid partition coefficient on n-hexadecane; parameters pertaining to the polymer include: r--the polarizability, s--the dipolarity, a--the hydrogen-bond basicity, b--the hydrogen-bond acidity, l--representing a combination of a negative term due to solvation cavity effects and a positive one due to dispersion interactions. The coefficients in Eq. 10 are determined by multiple linear regression analysis from a representative set of vapors in the polymer under study. These parameters have been tabulated for a large number of vapors and polymers [31].

The LSER approach has been criticized as being an empirical approach to predicting solvation. However, the fact that this approach has been used successfully to describe a variety of properties that depend on solute-solvent interactions suggests that it captures the essential features of solubility processes [1]. The fact that there are only five solute properties in Eq. 10 suggests that there are only a handful of relevant chemical properties that determine solubility in a physisorption-based absorptive coating.

The LSER method provides a rational approach to selecting a coating material to detect a

given analyte or set of analytes. This can be done by finding a polymer with functional groups that provide the right solubility interactions (LSER coefficients) for interacting with the target species. Ideally, one would like to maximize the solubility for the species of interest, while minimizing the solubility of interferents.

Using absorbent films, such as polymers, that have functional groups that interact with the analyte of interest typically leads to a significantly larger number of analytes being immobilized on the sensor surface (per unit area) than does a bare surface or monolayer coating. The equilibrium sensor response, S, is proportional to the partition coefficient K_p (see Eq. 10) and to film thickness, h. However, the equilibration time, τ, is typically much longer as species must diffuse into the film. The equilibration time for this diffusion process varies as h^2/D, where D is the diffusivity of the analyte in the film. Thus, for a given sorptive material, there is a tradeoff between sensitivity and speed of response in absorption-based sensors: $\tau \propto S^2$. The diffusivity is typically much higher in rubbery polymers than in glassy ones. For $h = 1$ μm, for example, a rubbery film (with $D \approx 10^{-8}$ cm^2/s) yields $\tau \approx 1$ s; a glassy film (D 10^{10} cm^2/s) yields τ 100 s.

Sensor Arrays

The solubility of vapors, for example in absorption-based polymer films, is typically not specific enough to a particular analyte to exclude interferants that may be present. One approach to solving this problem is to use an array of sensors, each coated with a different film, to resolve the chemical(s) present. This scheme is most successful when the set of films is "chemically orthogonal" in the sense that each emphasizes a different characteristic in the LSER equation (Eq. 10). Grate *et al.* have described a methodology for optimal film selection to resolve a given set

of analytes [31].

Fig. 10 illustrates how an array of three SAW chemical sensors, each with a different film, can be used to resolve a set of analytes. The normalized response from each sensor is displayed on an orthogonal axis. As the concentration of each analyte is varied, a locus of points is generated. Since the sets of points corresponding to each analyte are separated in space, they can be resolved. Several researchers have described pattern-recognition algorithm that can be used to categorize the data and identify an analyte [32].

Fig. 10 Three-dimensional plot of normalized responses to nine volatile organics for three SAW sensors coated with polyisobutylene (PIB), a flourinated siloxane ( ), and a cyanide-modified siloxane (SXCN).

Intuition might suggest that the larger the number of sensors included in an array, the better the discrimination capability. However, the LSER model outlined above indicates that absorption-based polymers have only five dimensions in which to work. Thus, limited benefit is obtained from arrays having more than five sensors, provided those five are chosen to be chemically orthogonal. Osborn *et al.* examined the discrimination of 10 analytes using all combinations from a set of 13 polymer films [33]. When significant error was added to the sensor responses, they found that the best discrimination was obtained using a subset of only six films. Adding more led to a degradation in identification accuracy. This is in general agreement with the conclusion drawn from the LSER model: having more films than there are distinct chemical characteristics is superfluous. In fact, it leads to a degradation in discrimination capability.

Sample Concentration and Separation

In many cases, the limit of detection is determined by sensor drift, generally attributable to sensor temperature changes. Significant improvement in detection levels can be achieved by incorporating an environmental sampling system that provides the sensor with chemical-free air to reestablish sensor baseline [34]. This can be accomplished with an adsorbent preconcentrator (Fig. 11) that consists of a section of tubing filled with an adsorbent material such as a porous polymer or a carbon-based compound. Samle gas is pumped through the preconcentrator and the analyte is "trapped" on the adsorbent. After a suitable accumulation period, a heater is used to increase the temperature to thermally desorb the analyte in a concentrated pulse. By loading from a large volume and desorbing into a smaller volume, sample concentrations of two to three orders of magnitude can be achieved [35]. An additional benefit, shown in Fig. 12, is that the chemical arrives at the sensor in a concentrated pulse so that a response peak can be easily identified above the sensor baseline response. Using a controlled temperature ramp of the preconcentrator, the difference in desorption temperatures results in some temporal separation of species arriving at the sensor. In Fig. 12, for example, the more volatile trichloroethylene (TCE) is released earlier (in separate runs) than perchloroethylene (PCE). This temporal separation can be used to improve chemical discrimination in the sensing system.

Fig. 11 Schematic showing components for preconcentrating analytes of interest and temporally separating them prior to detection.

Fig. 12 Response peaks due to thermal desorption of an adsorbent preconcentrator loaded with trichloroethylene (TCE) and perchloroethylene (PCE).

For analysis of individual components in complex mixtures, Wohltjen *et al.* [36] and Watson *et al.* [11] have shown that incorporating a chromatographic column greatly improves discrimination capability by fully separating the chemical species prior to detection. These columns separate species in time based on the relative time the analyte spends in the mobile phase (a gas flowing through the column) vs. the stationary phase (typically a thin layer that sorbs species to different extents, similar to polymeric sensor coatings described above). In some cases, such as detection of very low volatility compounds like explosives, an uncoated high frequency SAW resonator has been used and the compounds accumulate on the surface as they come out of the chromatographic column [11]. This results in the sensor acting as an integrator of the total amount of the analytes, as shown in the top curve in Fig. 13. Since the rate of change in the sensor response correlates with the concentration at the sensor, taking the derivative of the sensor data generates a curve showing peaks as each compound elutes from the column (this type of response, shown in the bottom curve in Fig. 13, is what is observed with typical gas chromatograph detectors). Alternatively, if the analyte sorbs rapidly and reversibly, the sensor response will look like the bottom curve in Fig. 13 since the sensor response tracks the concentration as a function of time [36]. These systems can provide identification and quantitation of many compounds in simple mixtures and, based on optimizing the system for fast analysis, can still provide results in 10 - 15 sec [11].

Fig. 13 Chromatographic separation with an acoustic sensor as the detector.

Sensor Integration

There are several advantages that result from sensor integration, including (1) improved signal-to-noise ratios due to reduction in electrical parasitics, (2) improved signal conditioning due to on-chip electronics, (3) reduced incremental cost from batch fabrication, (4) reduced size and power requirements, (5) faster response, and (6) greater reliability due to reduction in bond wires and package count. Typically, the main driver to integrate sensors is economic. The large initial cost to develop an integrated sensor can be offset by the reduced incremental production cost if a large number of sensors is produced.

There are also several disadvantages or difficulties that arise from sensor integration. The sensor development time and cost is typically increased, since greater constraints are placed on the sensor design and processing. The yield for an integrated sensor is typically lower, since both the sensor and associated electronics must be made to operate simultaneously. Material compatability is typically a problem, since many sensing materials will "poison" the IC process. Packaging is typically more difficult for an integrated sensor since the sensor must be exposed to the environment, while the electronics are typically protected in an inert environment. Sensor interchangeability is also an issue, since changing the sensor requires replacing the electronics also. Finally, since microelectronic circuits typically cannot operate at high temperatures, this sets temperature limitations on the sensor operation.

Table I lists a number of acoustic devices that can be used to make an integrated gas/vapor sensor, along with some of the attributes relevant to integration. A primary consideration in selecting an acoustic sensor for gas or vapor detection is the mass sensitivity. By concentrating

acoustic energy in a thin film, the monolithic bulk resonator and FPW devices are clearly superior in this regard. A second consideration is the operating frequency. Typically the microelectronic processing capabilities available set an upper limit on the frequency for which oscillator electronics can be constructed. In this regard, the hybrid resonator, FPW, cantilever beam and comb-drive resonator are superior. To realize a low detection limit, oscillator stability is a prime consideration. Resonant devices with high Q-values have narrow bandwidths and yield greater oscillator stability. The hybrid and monolithic bulk resonators, as well as the SAW resonator, yield high device Qs. The FPW resonator exhibits moderate Q-values.

Table I. Comparison of acoustic sensor attributes pertaining to integration on silicon. Mass sensitivity is given in terms of fractional frequency shift per areal mass density deposited.

Device	*Typical frequen. (MHz)*	*Mass Sensitiv. (cm^2/g)*	*Q-value in air*	*IC Compat-ibility*	*Temp. Stability*	*Rugged-ness*	*Packag-ing*	*Coata-bility*
Bulk reson. on Si	*1,000*	*1,000*	*1,000*	*Poor*	*Medium*	*Medium*	*Medium*	*Good*
SAW delay line	*100*	*90*	*NA*	*Medium*	*Good*	*Good*	*Medium*	*Good*
SAW resonator	*100*	*90*	*10,000*	*Medium*	*Good*	*Good*	*Medium*	*Good*
FPW (piezo)	*2.6*	*1,000*	*?*	*Poor*	*Poor*	*Poor*	*Good*	*Medium*
FPW (mag)	*0.5*	*1,000*	*1,000*	*Medium*	*Poor*	*Poor*	*Good*	*Medium*
Cantilever-beam	*0.014*	*~1,000*	*~1*	*Good*	*Poor*	*Medium*	*Medium*	*Poor*
Comb drive	*0.005*	*~1,000*	*~1*	*Good*	*Poor*	*Medium*	*Medium*	*Poor*

Other considerations in integrating sensors are material and process compatability with the integrated circuit (IC) process. Due to the fact that piezoelectric films typically involve elements (e.g, Zn) that are Si dopants, devices that involve piezoelectric films are problematic if further processing is required after film deposition. Thus, the monolithic bulk resonator, SAW, and FPW devices, that require piezoelectric films for wave excitation, are at a disadvantage in comparison with devices such as the magnetically-excited FPW and electrostatically-driven cantilever beams and comb-drive resonators. Ideally, fabrication of the sensing device would involve only the processing steps required to produce the integrated electronic circuitry, for example, a CMOS process. However, typically some additional processing steps are required such as a backside etch in the case of bulk-micromachined devices (monolithic bulk resonator and bulk-micromachined FPW devices) or removal of a sacrificial oxide layer in surface-micromachined sensors (surface-micromachined FPW device, cantilever beam, comb-drive resonator). The surface-micromachining process leverages the integrated circuit industry more effectively, i.e., takes advantage of existing equipment and processes better [37]

Another consideration in achieving a stable oscillator is to minimize temperature drift. Thus, temperature stability is a prime consideration. The SAW and monolithic bulk resonator can be made reasonably temperature stable by incorporating the proper thickness of SiO_2. The micromachined devices (FPW, cantilever beam, and comb-drive resonator) are probably the least temperature stable.

There are other considerations, such as device ruggedness that must also be considered in

some applications. The monolithic bulk resonator and FPW devices both use very thin membranes that are typically under tension. These devices, particularly the larger FPW device, tend to be more fragile than devices constructed on monolithic substrates.

Other considerations, such as sensor area and assembly, impact the cost of producing an integrated sensor. Sensor cost is reduced if the sensor area is very small and many devices can be produced per wafer. The SAW resonator, in contrast, includes reflector arrays that occupy a large area (on low frequency devices). This may make it uneconomical to integrate.

Some final considerations include how easily the device can be coated with a sensing film and packaged. Devices whose sensing area lies on a planar surface, such as the SAW and monolithic bulk resonator, are most easily coated. On the other hand, devices in which the excitation electronics and sensing surface are on opposite sides, such as the bulk-micromachined FPW device, can be easily packaged in a way that exposes the sensing film while protecting the microelectronics. There seems to be a compromise between these two considerations.

While some general conclusions can be drawn from the comparison in Table I, the relative merit of these considerations depends on the processing capabilities and the particular application. For high sensitivity in integrated gas/vapor sensors, the high sensitivity at low operating frequency (compatible with CMOS drive electronics) obtained from FPW devices is very attractive. FPW resonators, with Q-values near 1000, are even more attractive due to their promise of greater stability. The material and process compatability of the bulk-micromachined devices with piezoelectric films, however, is not very good. This could be improved by (1) using either AlN films or magnetic excitation and (2) using surface-micromachining techniques to fabricate the suspended membrane. The temperature stability and durability of these devices may preclude their

use for some applications. The SAW resonator, while requiring fairly high operating frequency to obtain good mass sensitivity, also scores well due to it's high Q-value, good temperature stability, ruggedness, and coatability. The high frequencies favor integration on GaAs (over Si) due to its higher carrier mobility.

Sensor Scaling

As fabrication processes are developed to make devices smaller, the question arises as to how scaling affects sensitivity. Some devices, such as accelerometers, are adversely affected by scaling down their size: If we consider scaling down a given accelerometer geometry, with characteristic dimension l, we find the proof mass m scales as l^3, while the spring constant k (from a beam, for example) scales as l^2. As l is reduced, the deflection arising from a given acceleration, proportional to m/k and scaling as l, is reduced, i.e., the sensitivity is reduced proportionately with linear dimension. Likewise, a spectroscopic chemical detector, whose signal is proportional to path length, experiences a similar degradation in sensitivity as device dimension is scaled down.

The sensitivity of an acoustic chemical sensor, on the other hand, is generally improved by scaling down the size. The actual gain depends on the application and whether you are (1) concentration limited, or (2) sample limited. In either case, the acoustic sensor's response is proportional to the mass per area (Eqs. 1 - 4), rather than absolute mass.

Concentration limited In most applications there is adequate gas phase sample to be collected and detection is limited by the concentration of species. At a given concentration, the mass per area accumulated on the surface is proportional to the partition coefficient K_a (an intrinsic property) and

the film thickness h. Considering the SAW device in an oscillator circuit, for example, $\Delta f \propto f_o^2 h$. In order to maintain a constant attenuation, h must be scaled inversely with frequency, i.e., $h \propto 1/f$, resulting in $\Delta f \propto f_o$. Since f_o scales inversely with the transducer periodicity (or characteristic length l), we have $\Delta f \propto 1/l$. This indicates that sensitivity *increases* inversely with linear dimension in the concentration-limited regime.

Sample limited In some applications, such as explosive detection, one has only a limited time or volume in which to collect a sample. The best one can do is concentrate this sample, with total mass M', and deposit it all on the active area (l^2) of the sensor, giving a surface mass density $\rho_s = M'/l^2$. Again considering the SAW device, the response is $\Delta f = -c_m f_o^2 M'/l^2$ or $\Delta f \propto f_o^4$. Since $f_o \propto 1/l$, we find that $\Delta f \propto 1/l^4$. Thus, in the sample-limited regime, sensitivity increases inversely with the *fourth* power of device linear dimension [38]. The scaling down of acoustic chemical sensors is advantageous; how much so depends on the application and sampling regime.

Conclusions

Acoustic devices are very sensitive gravimetric detectors that serve as versatile platforms for a wide range of gas and vapor sensors. These devices generally respond to the mass density of species immobilized on their surface. This immobilization is effected by various means, including surface monolayer treatments, high surface area films, and absorptive films. Generally, weak physical interactions between the surface and analytes results in non-specific but reversible binding; strong chemical interactions are more specific but generally irreversible. There are several approaches to increasing sensor discrimination, including using arrays of sensors combined with a pattern-recognition algorithm. For arrays, it is important to choose films that are

chemically orthogonal. Since there are only a limited number of chemical interactions in absorptive polymer films, there is a similar number of sensors that will provide optimum discrimination.

Another approach for improving discrimination is to effect a separation of species. This is typically done with preconcentrators and chromatographic columns. Temporal separation is especially effective for mixtures of gases. To make sensor systems smaller and cheaper, the trend is to fabricate them on silicon or GaAs and include integrated electronics. There are a number of acoustic sensors that have been developed to be integrable on semiconductor substrates. These devices have various advantages and disadvantages with regard to sensitivity, operating frequency, Q-value, process compatibility, and robustness. The device of choice will depend critically on the application. Scaling these sensors to smaller size favorably affects their sensitivity.

Acknowledgments

The authors are grateful to M. W. Scott, R. W. Cernosek, J. H. Smith, G. C. Osbourn, A. J. Ricco, and J. W. Bartholomew of Sandia National Laboratories (SNL) for technical discussions, as well as to K. Rice of Team Specialty Products for technical assistance. This work was supported by the United States Department of Energy under Contract DE-AC04-94AL85000. Sandia is a multiprogram laboratory operated by Sandia Corporation, a Lockheed Martin Company, for the United States Department of Energy.

References

[1] D. S. Ballantine, R. M. White, S. J. Martin, A. J. Ricco, G. C. Frye, E. T. Zellers, and H. Wohltjen, *Acoustic Wave Sensors: Theory, Design, and Physico-Chemical Applications* (Academic Press, New York, 1997).

[2] M. S. Nieuwenhuizen and A. Venema, *Sensors and Materials*, **5**, 261-300 (1989).

[3] W. H. King, *Anal. Chem.* **36**, 1735 (1964).

[4] G. Sauerbrey, *Z. Phys.* **155**, 206-222 (1959).

[5] S. J. Martin and G. C. Frye, *IEEE Ultrason. Symp. Proc.* (IEEE, New York, 1991) 393-398.

[6] J. H. Smith and S. D. Senturia, *Digest of Technical Papers*, Transducers 95, Eurosensors IX, Stockholm, Sweden, June 1995, Vol. 2, 724-727.

[7] K. M. Lakin, G. R. Kline, and K. T. McCarron, *IEEE Trans. on Microwave Theory and Techniques*, **41**, 2139-2146 (1993).

[8] R. M. White, *Proc. IEEE*, **58**, 1238-76, (1970).

[9] S. J. Martin, G. C. Frye, and S. D. Senturia, *Anal. Chem.*, **66**, 2201- 2219 (1994).

[10] S. J. Martin and A. J. Ricco, *IEEE Ultrason. Symp. Proc.* (IEEE, New York, 1989) 621-625.

[11] G. Watson, W. Horton, and E. Staples, *IEEE Ultrason. Symp. Proc.* (IEEE, New York, 1992) 269-73.

[12] S. W. Wenzel and R. M. White, *IEEE Trans. Electron Devices*, **ED-35**, 735 (1988).

[13] M. J. Vellekoop, "A Smart Lamb-Wave Sensor System For The Determination Of Fluid Properties," PhD Thesis, Electrical Engineering Department, Delft University Of Technology, (Delft University Press, 1994) 61-63.

[14] M. Viens, P. C. H. Li, Z. Wang, C. K. Jen, M. Thompson, and J. D. N. Cheeke, *IEEE Ultrason. Symp. Proc.* (IEEE, New York, 1993) 359-364.

[15] T. Thundat, G. Y. Chen, R. J. Warmack, D. P. Allison, and E. A. Wachter, *Anal. Chem.* **67**, 519-521 (1995).

[16] J. J. Sniegowski, "Design and fabrication of the polysilicon resonating beam force transducer," Ph.D. Thesis, Dept. of Electrical Engineering, Univ. of Wisconsin, 1991.

[17] W. C. Tang, T. C. H. Nguyen, and R. T. Howe, IEEE Micro Electromechanical Systems Workshop, Salt Lake City, Utah, Feb. 20-22, 1989, 53-59.

[18] A. W. Adamson, *Physical Chemistry of Surfaces*, 4th Edition (Wiley, New York, 1982).

[19] A. J. Ricco, L. J. Kepley, R. C. Thomas, L. Sun, and R. M. Crooks, *Technical Digest*, IEEE Solid-State Sensor and Actuator Workshop, Hilton Head Island, SC, June 22-25, 1992, 114-17.

[20] G. C. Frye, C. J. Brinker, A. J. Ricco, S. J. Martin, J. Hilliard, and D. H. Doughty, *Mat. Res. Soc. Symp. Proc.*, **180**, 583-93 (1990).

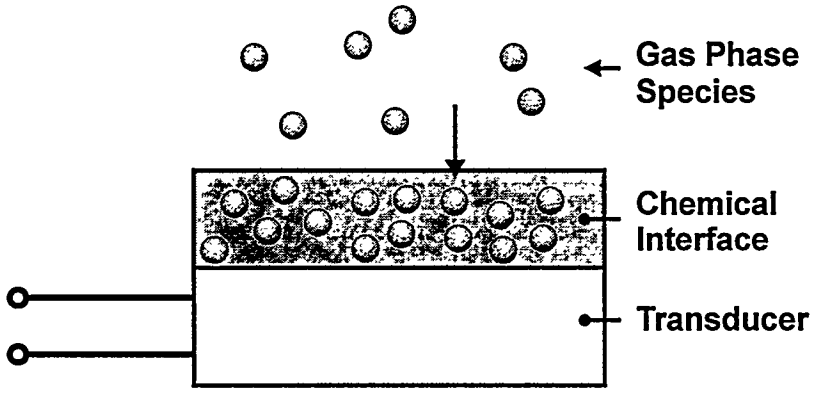

Fig. 1

kar:1315:f:\steve\wuadfcs.cdr-dd3:10/96

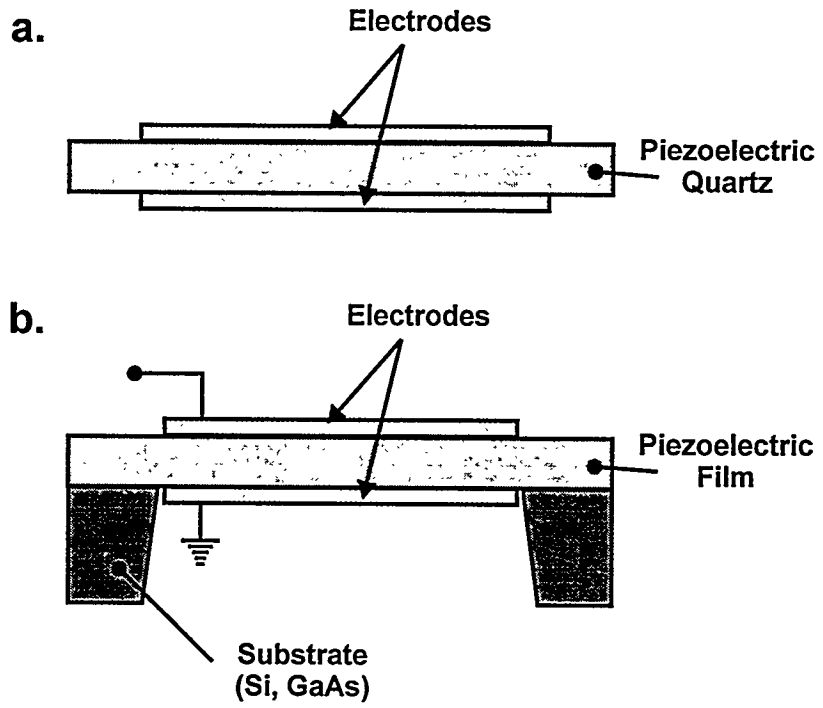
a.
Electrodes
Piezoelectric
Quartz
b.
Electrodes
Piezoelectric
Film
Substrate
(Si, GaAs)

Fig. 2

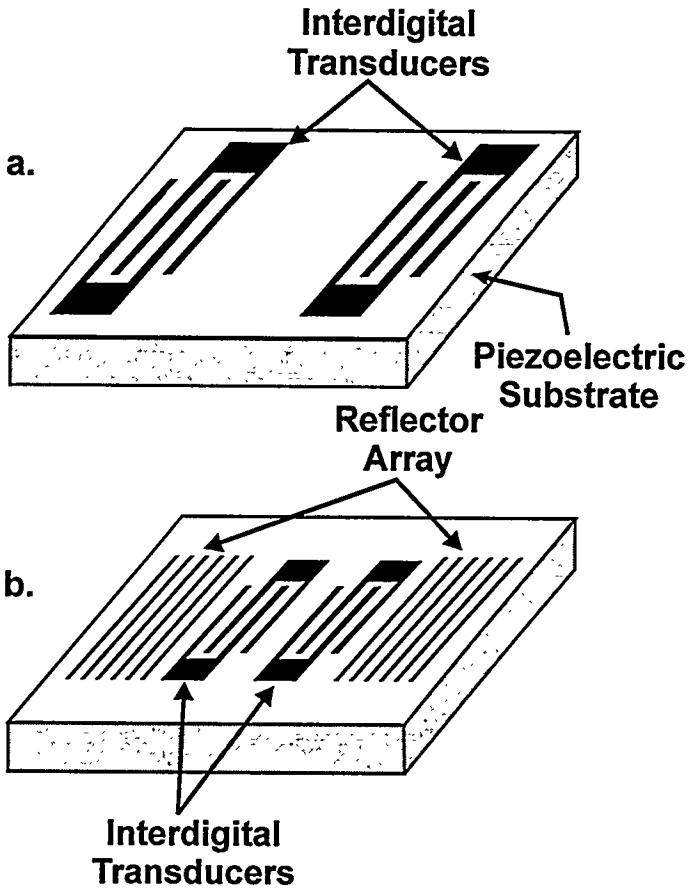

Fig. 3

kar:1315:steve/saw(saw)s.cdr-dd3:10/96

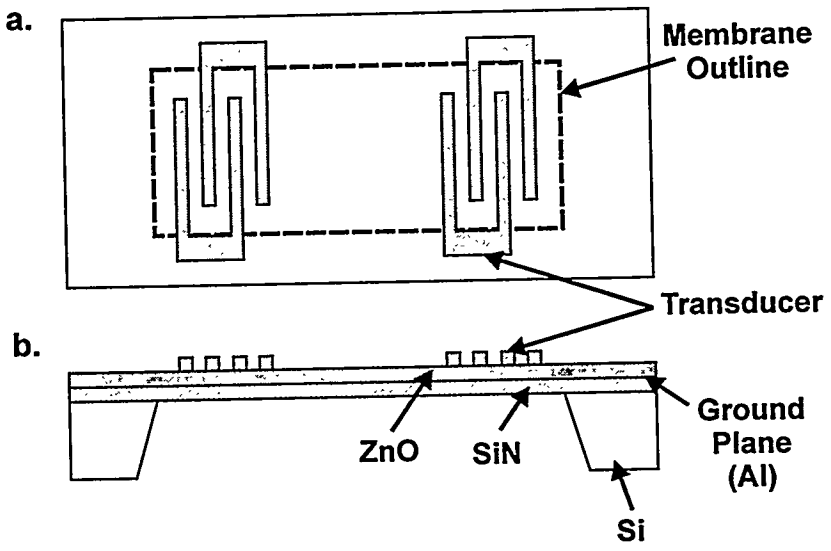

Fig. 4

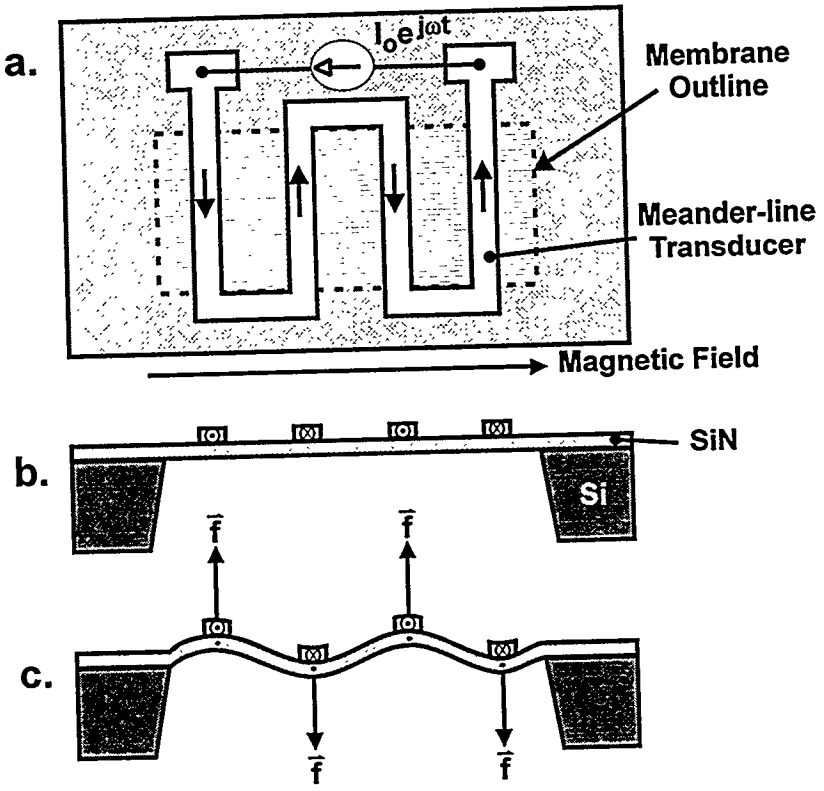
a.
$I_o e^{j\omega t}$
Membrane
Outline
Meander-line
Transducer
Magnetic Field
b.
SiN
Si
c.
$\vec{f}$
$\vec{f}$
$\vec{f}$
$\vec{f}$

Fig. 5

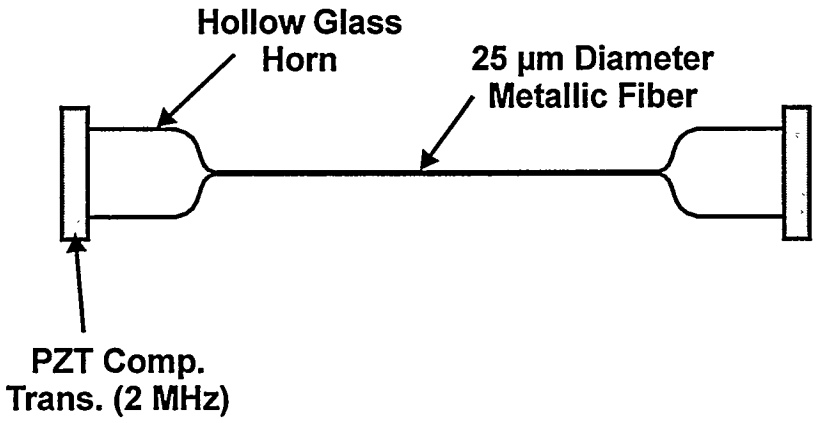
Hollow Glass
Horn
25 µm Diameter
Metallic Fiber
PZT Comp.
Trans. (2 MHz)

Fig. 6

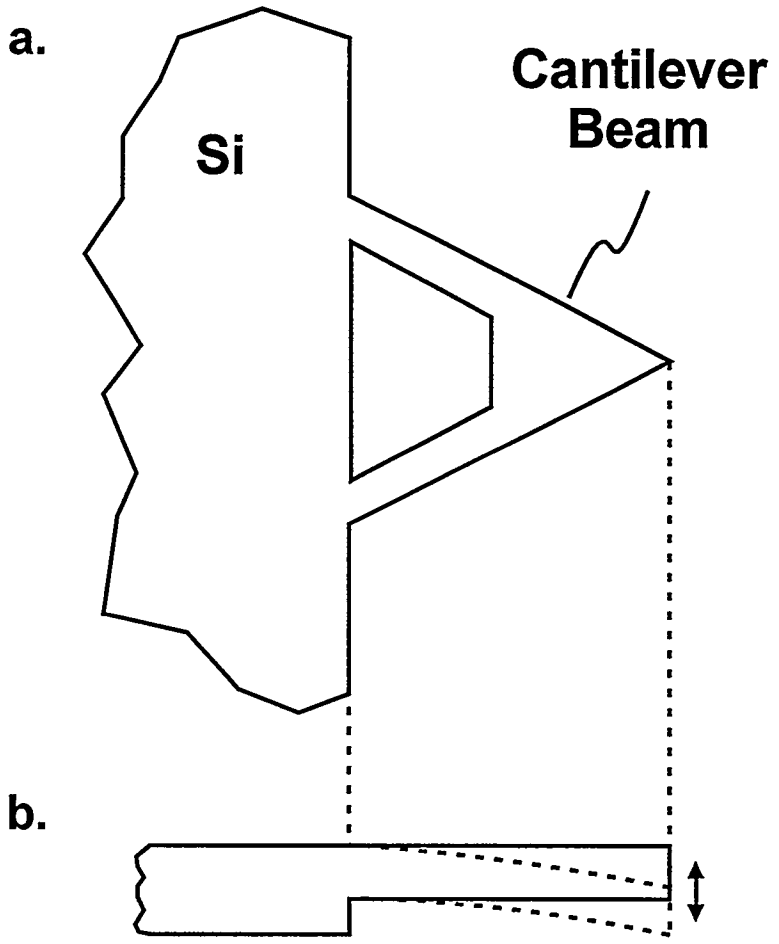

Fig. 7

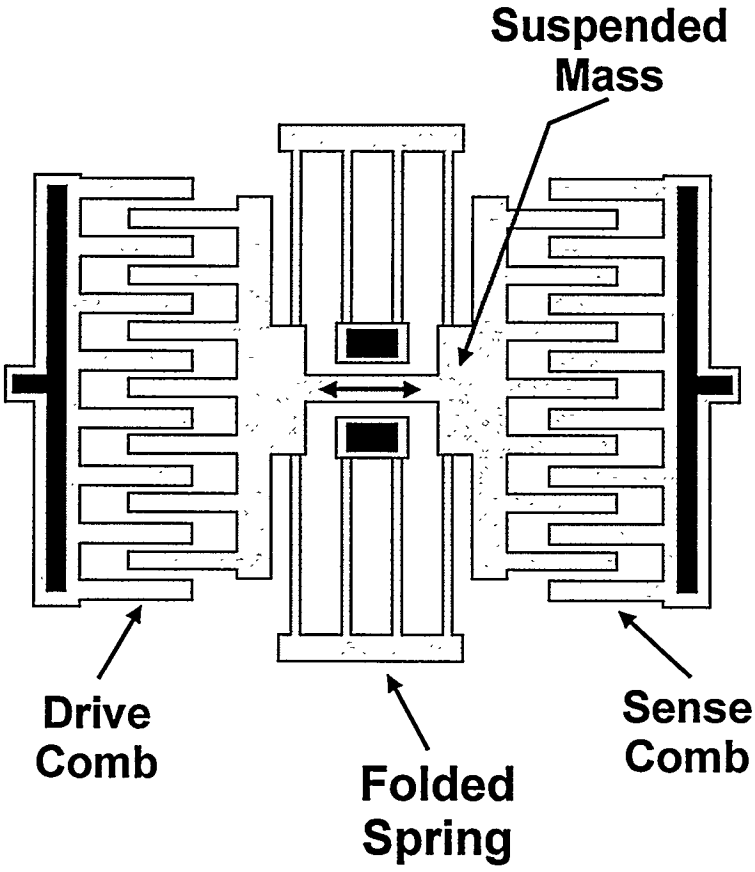

Fig. 8

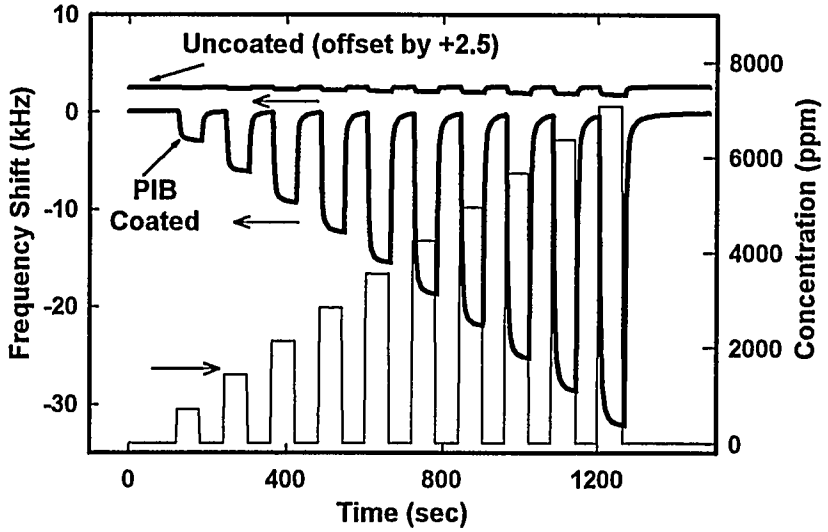

kar:1315:greg\plbvsunc.jnb:11/96

Fig. 9

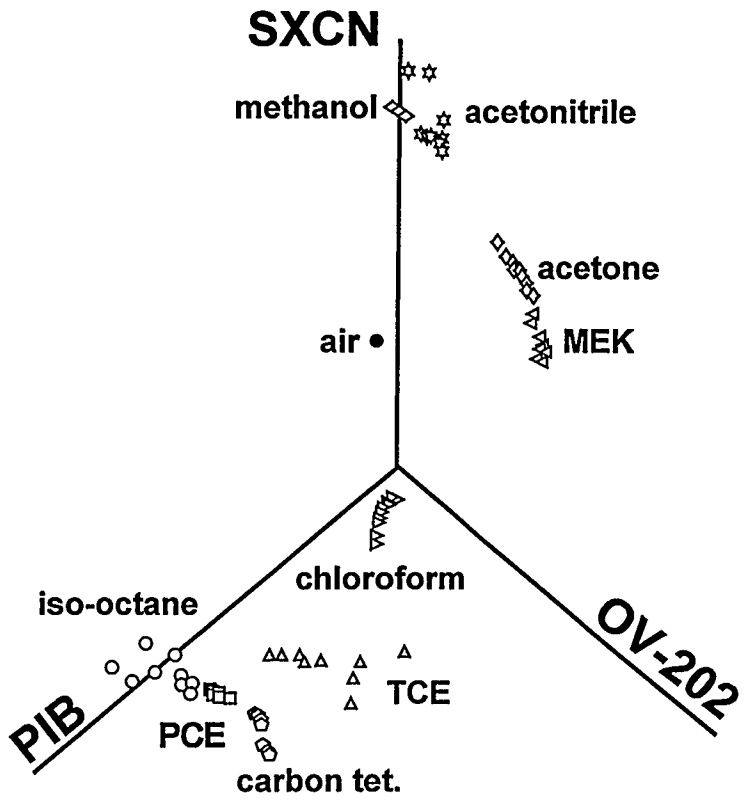
SXCN
methanol
acetonitrile
acetone
air
MEK
chloroform
iso-octane
OV-202
TCE
PIB
PCE
carbon tet.

Fig. 10

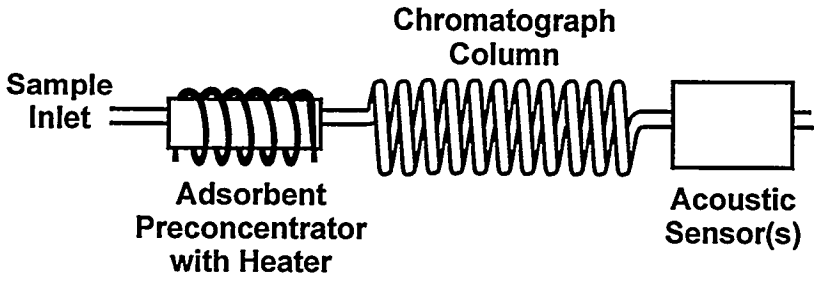

Fig. 11

kar:1315:f:\greg\coils.cdr-dd3:10/96

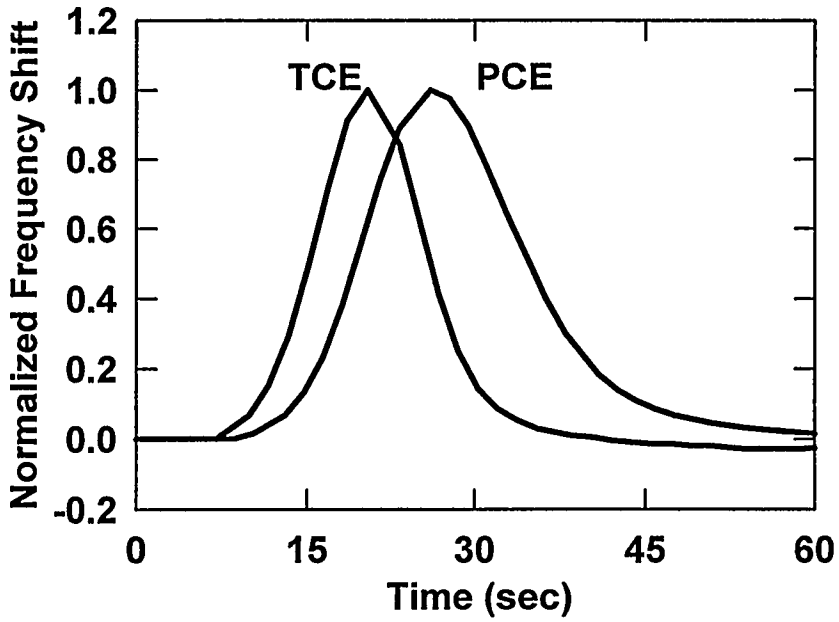
Normalized Frequency Shift
1.2
1.0
0.8
0.6
0.4
0.2
0.0
-0.2
TCE
PCE
0
15
30
45
60
Time (sec)

Fig. 12

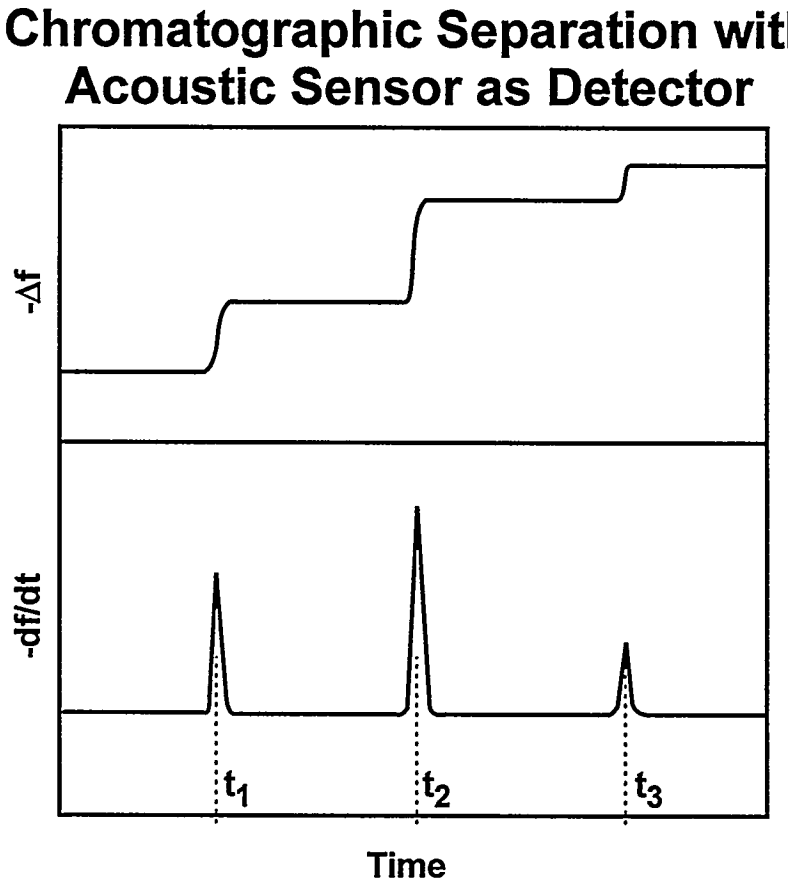
Chromatographic Separation with
Acoustic Sensor as Detector
-Δf
-df/dt
t1
t2
t3
Time

Fig. 13